Activities of AR & DB Associate Centre for CFD at IIT Kanpur

T. K. Sengupta* & Sanjay Mittal†
Department of Aerospace Engineering
Indian Institute of Technology
Kanpur 208 016
INDIA

INTRODUCTION

With the advent of faster computers with large memory, CFD is gaining in importance for complete aircraft design cycle. For example the external configuration of Boeing 777 wide-body subsonic transport was designed utilisiing CFD tools that minimised viscous and shock losses at transonic speed via the usage of coupled potential flow methods along with interactive boundary layer codes and this is discussed in Rubbert [1]. *Off-design performance associated with maximum lift, buffet and flutter, and the determination of stability and control derivatives, involving unsteady separated and vortical flows with stronger shock waves, are determined largely by experimental methods. Computational simulations of these flow fields requires the use of Reynolds-Averaged Navier-Stokes (RANS) methods; these computations for high-Reynolds flows over complex geometries are very expensive... and the turbulence models for separated flows have a high degree of variability. Thus in these areas experiments, rather than computations, are preferred for reasons of cost and uncertainty.* [2]

The CFD activities at IIT Kanpur were given an impetus with the formation of the centre with support from ARDB. Immediately after the formation of the centre, a special meeting identified the areas of work for the various centres [3]. For the centre at Kanpur, it was suggested that the area of unsteady aerodynamics in general and decelerator aerodynamics in particular be the focus of activity. Following is a brief description of various activities of the centre at Kanpur.

1 High Angle of Attack Aerodynamics(2D):

Some efforts have been made in this area related to unsteady aerodynamics by solving Navier-Stokes equation with and without turbulence models. Finite difference (FD), finite volume (FV) and finite element (FE) methods are currently in use. The FD and FV methods are based on higher order upwinding and interpolation of fluxes repsectively.In the following the FE method results are reported with and without turbulence closure, while for FD and FV methods no turbulence models have been used since these are with higher spectral accuracy and can resolve much higher wave numbers and frequencies. The results for FD methods are with higher order upwind methods for incompressible flows and we have investigated the static and dynamic stall of aerofoils, effect of flow acceleration/ deceleration and other additional strain effects [4]. Dynamic stall studies are important for helicopter aerodynamics. We have also studied the flow control aspect for high angle of attack cases. A simple algebraic turbulence model (Baldwin Lomax model) to be used with the finite element Navier-Stokes solver on unstructured is also developed. Figure 1a shows one such result for a NACA 0012 airfoil at $\alpha = 10^o$ and $Re = 10^6$. Computations at other angles of attack have been carried out and show that the flow ceases to be steady at approximately $\alpha = 15^o$. Figure 1b shows the effect of flow establishment process at moderate Reynolds number at high angle of attack with different type of acceleration using the FD higher order upwinding method. The agreement of our computation (case IV) with the experiment of Morikawa & Gronig is good and has been

†Assistant Professor
*Associate Professor

reported at seventh ACFM. Figure 2 shows the solution for a post-stall angle ($\alpha = 20^o$. Figure 3 shows the loads and pitching moment experienced by an elliptic aerofoil for a moderate and high frequency oscillation. Both the case exhibit deep dynamic stall. The computational results are obtained by solving Navier- Stokes equation by a fifth order upwinding method [4].

Figure 4a shows a case where the effect of control can be observed at $Re = 10^4$ which has been computed by the FE method. The unsteadiness in the flow is significantly reduced and the drag coefficient reduces to 0.27. Figure 4b shows the control of unsteadiness by a rotating nose portion of a NACA 0012 airfoil for $\alpha = 20^o$ and $Re = 46,200$ - these parameters corresponds to the experimental results obtained by Modi et al [5]. The results corresponding to our Model 4 matches with the experimental trends and these are obtained by solving Navier- Stokes equation using a (233 X 300) grid for the third order upwind method that uses skew symmetric differencing to reduce aliasing errors.

2 Wing Aerodynamics (3D):

For this exercise a compressible flow code for Navier-Stokes equation was developed utilising finite element method based on SUPG formulation. Figure 5 shows the computed $M = 0.84$ and $Re = 1.2X10^7$ flow past the ONERA M6 wing at $\alpha = 3.03^o$. A modified Baldwin Lomax turbulence model has been utilized for the computations. A lambda shock can be observed on the upper surface of the wing. The pressure distribution is in good agreement with results from other researchers.

3 Flows Past Cascades:

Here we have developed a time accurate finite volume method to solve compressible Navier- Stokes equation for flow past cascades. Flux vector splitting has been used utilising higher order interpolation scheme for spatial discretization. For time marching rational Runge Kutta method has been used. The results for Double Circular Arc (DCA) cascade have been computed and they are being validated with standard AGARD report results. This is a time accurate method and some results for initial times are shown in Figure 6.

4 Decelerator Aerodynamics:

The main impetus in this area comes from an ARDB sponsored project and the requirements of ADRDE, Agra. The FE method is used to study the performance of a Ram Air Parachutes. Figure 7 shows the Navier-Stokes solution for $Re = 10^6$ flow past ram air parafoil at $\alpha = 0^o$ with Baldwin- Lomax closure model. Flow within and outside the parafoil is simulated. The formulation allows for a pressure jump across the parachute membrane. The effect of angle and location of the cut at the leading edge is being investigated. It is observed that at low angles of attack, because of the sharp cut, the flow separates right at the leading edge and results in unsteadiness of the aerodynamic forces.

5 Other Related CFD Activities:

a) Flows through supersonic diffusers:

Supersonic wind tunnel flow have been simulated for DSC, Delhi for their effort in designing a diffuser section for a gas-dynamic laser. A stabilized FE formulation is employed to compute viscous flows in supersonic diffusers. The conservative form of Navier-Stokes equation are solved on unstructured meshes. The accuracy of the basic method has been increased by the Enhanced-Discretization Interface-Capturing Technique (EDICT) specifically developed recently for unsteady flow simulation. Figure 8 shows the flow through a supersonic wind tunnel with a stagnation to exit pressure ratio of 25. The interaction of the oblique shocks and the boundary layer is quite apparent in the diffuser section. The figure also shows the effect of mesh refinement using EDICT.

b) Fluid-Structure Interaction:

Flows past multiple bluff bodies have been investigated for a DST sponsored project. In this context the free vibration of single and two-cylinder configuration has been studied. The two cylinder configuration is either in tandem or in staggered configuration. Both in-line and transverse vibration cases have been investigated. Figure 9 shows the Navier- Stokes solution for flow past two oscillating cylinders that are initially in tandem arrangement. The downstream cylinder lies in the unsteady wake of the upstream one and exhibits larger amplitude oscillations. For single cylinder, a static control cylinder has been found effective in suppressing shedding at low Reynolds number. At high Reynolds numbers two contra-rotating control cylinders at the shoulder and at the bottom was found to be effective in flow control.

6 Transitional Flows:

We have started investigating transitional flows over airfoil and infinite swept wings. The aim is to study the effect of free stream turbulence and vibration on transition. In this context we have also worked on noise modelling and characterised the resultant flows by various dynamical system tools. While the effect of vibration is already studied by solving linearized Navier- Stokes equation by spectral method, the effect of free stream turbulence is studied by solving the unsteady full Navier- Stokes equation by the third order upwind method. Figure 10 shows some representative results for flow past a NACA 0015 airfoil for $\alpha = 30^o$ and $Re = 10^5$ at a point just downstream of the trailing edge.

7 Numerical Methods:

This is an important area related to its potential application for DNS and LES. The developed higher order upwind methods requires their performance evaluation with respect to other commonly used methods. In Figure 11, we show some performance characteristics of different upwind and central schemes. High Reynolds number flows that has to be simulated should not suffer from spurious dispersion and at the same time should have high spectral resolution. The combination of these are shown in Figure 11.

References

[1] RUBBERT P.E. 1994 CFD and the changing world of airplane design. *AIAA Wright Brothers Lecture* Anaheim California.

[2] BRANDT ACHI 1998 Barriers to achieving textbook multigrid efficiency in CFD *NASA/CR*-**1998-207647**

[3] Minutes of the 1st SPC meeting of AR & DB Centre of Excellence in Aerospace CFD held at JATP on 20th May 1997.

[4] MANOJ T. NAIR 1998 Accurate Numerical simulation of Two - Dimensional Unsteady Incompressible Flows. Ph. D. thesis (submitted) Dept. of Aerospace Engineering, IIT Kanpur May 1998.

[5] MODI V.J., MOKHTARIAN F., FERNANDO M.S.U.K. & YOKOMIZO T. 1991 Moving Surface Boundary-Layer Control as Applied to Two-Dimensional Airfoils. *J. of Aircraft* **28** pp 104- 112.

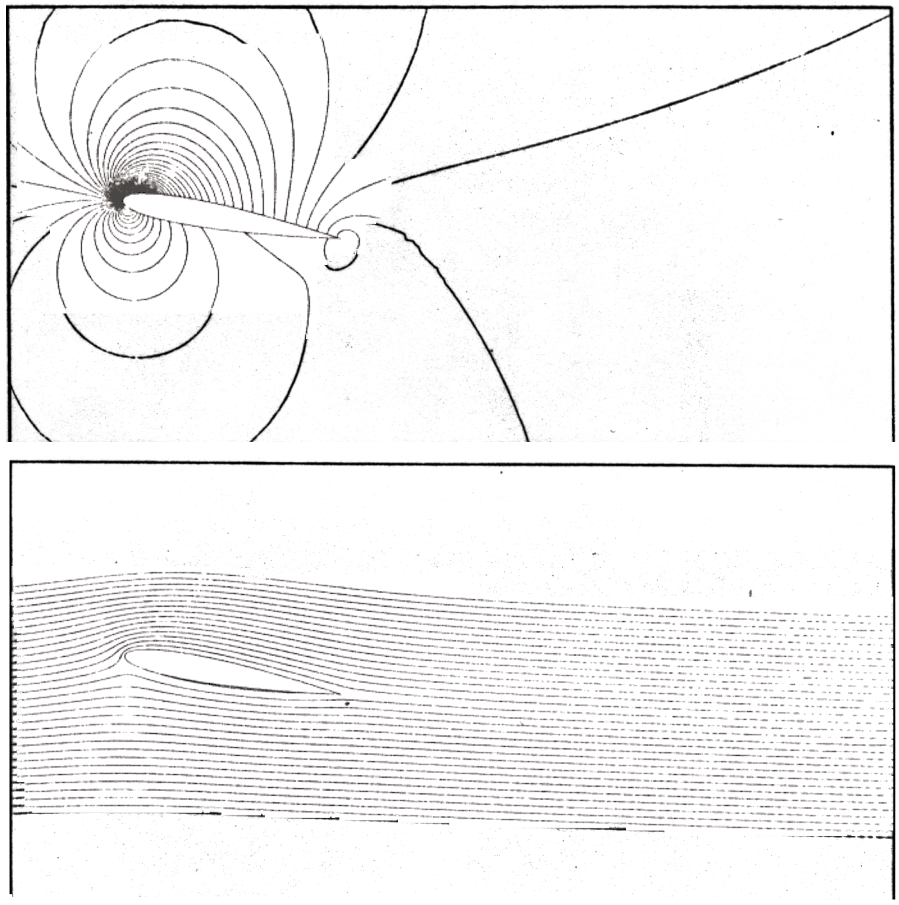

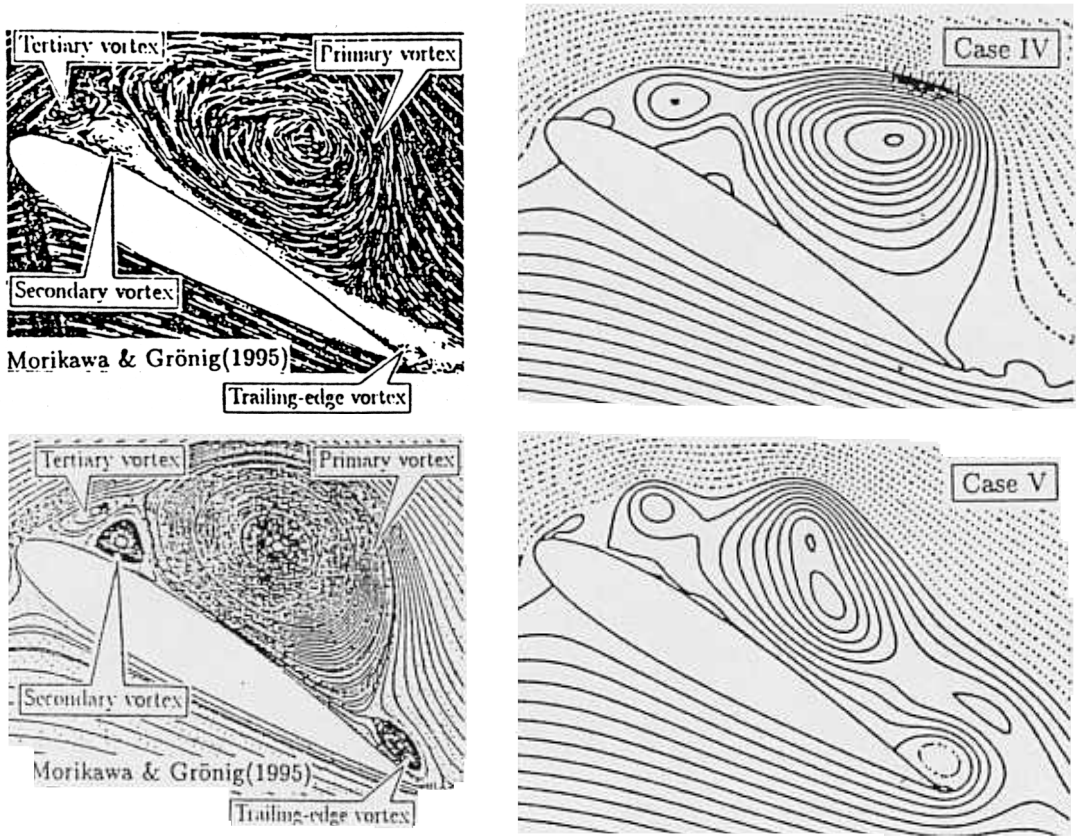

Figure 1. Navier- Stokes solution for high α airfoil aerodynamics: a) NACA 0012 at $\alpha = 10^o$ with Baldwin- Lomax closure model ($Re = 10^6$) b) Accelerated flow past NACA 0015 aerofoil for $\alpha = 30^o$ at $Re = 35000$. LHS- expt. & computation by Morikawa & Gronig. RHS- present computations. Case IV- uniform accelerated start; Case V- impulsive start.

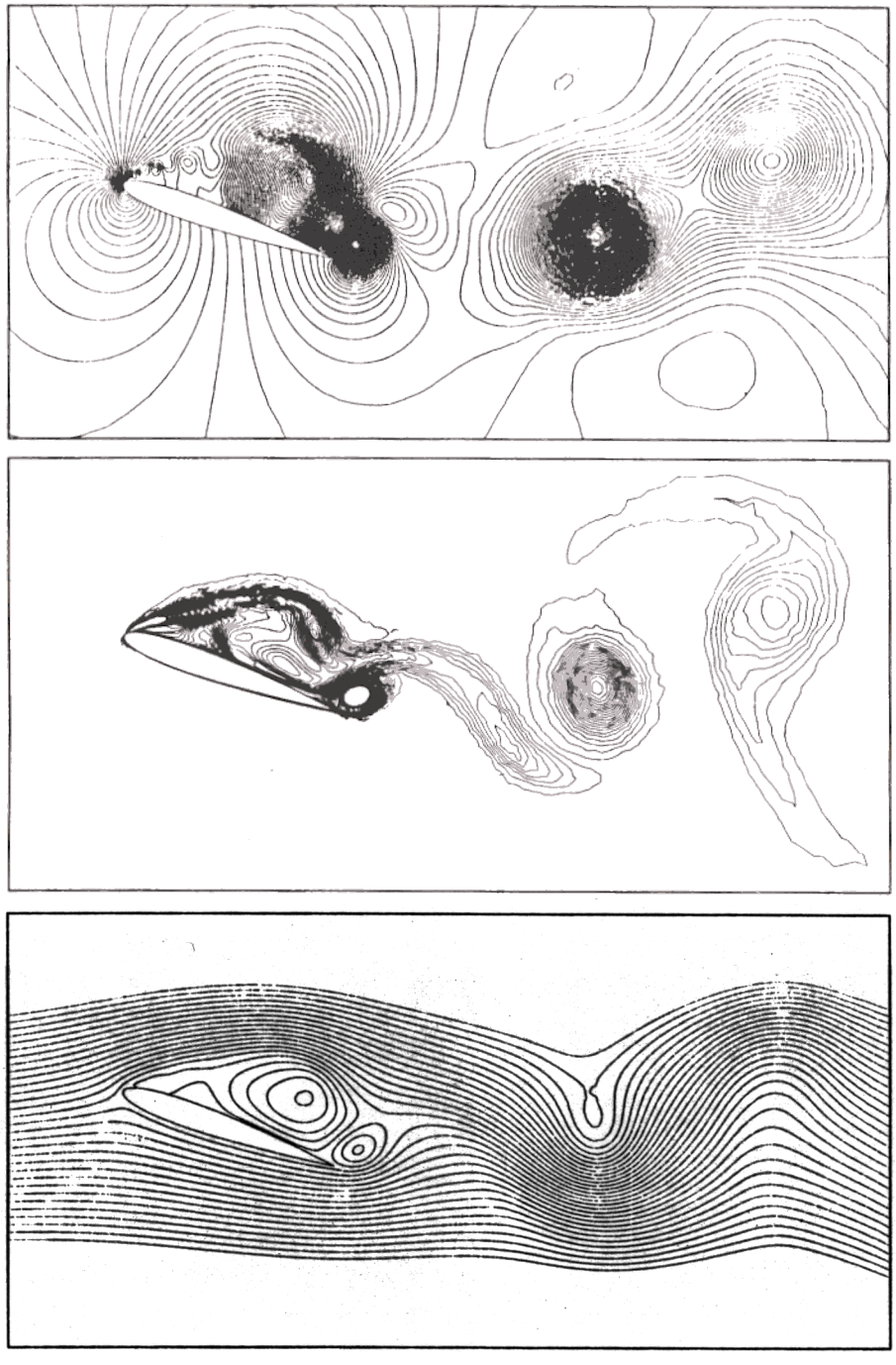

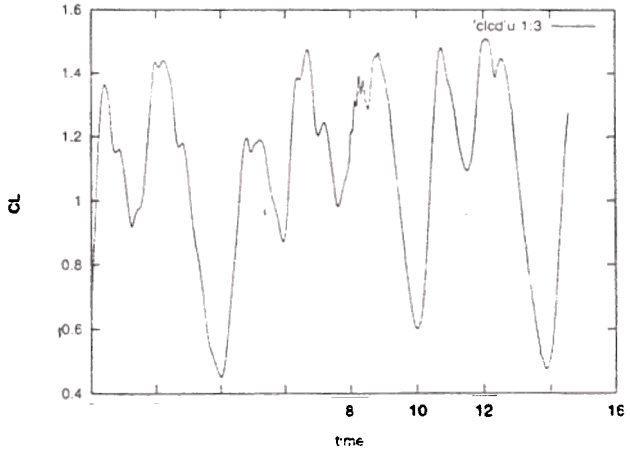

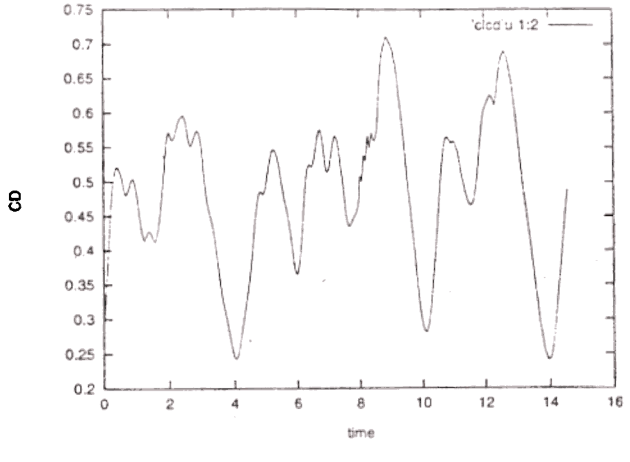

Figure 2. Navier- Stokes solution for high α airfoil aerodynamics: NACA 0012 at $\alpha = 20^o$ with Baldwin- Lomax closure model ($Re = 10^6$)

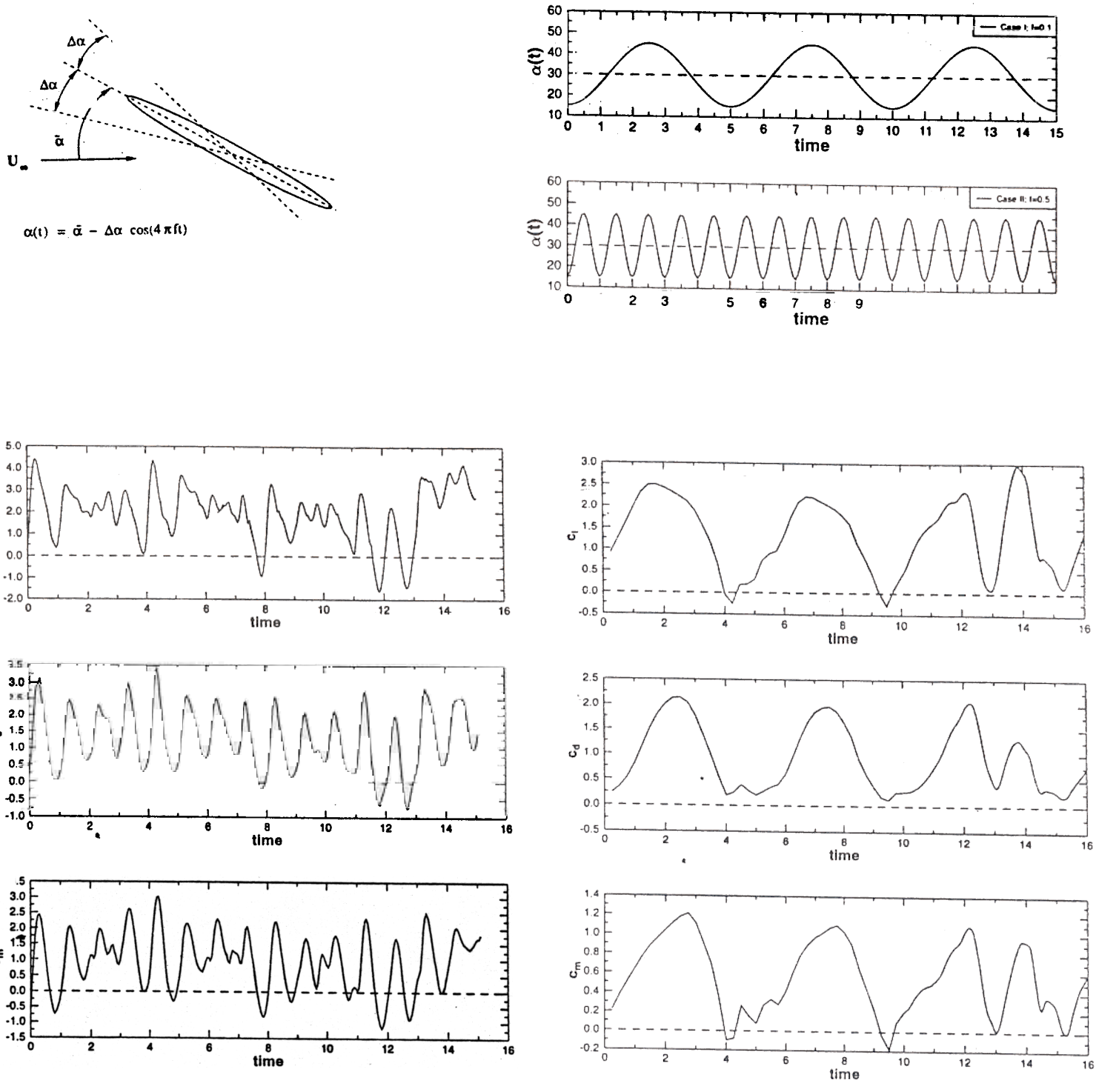

Figure 3. Loads and pitching moment during dynamic stall of elliptic aerofoil at $Re = 3000$ for oscillation frequencies a) $f = 0.1$ & b) $f = 0.5$. For both the cases $\alpha = 30^o$ and oscillations of 15^o.

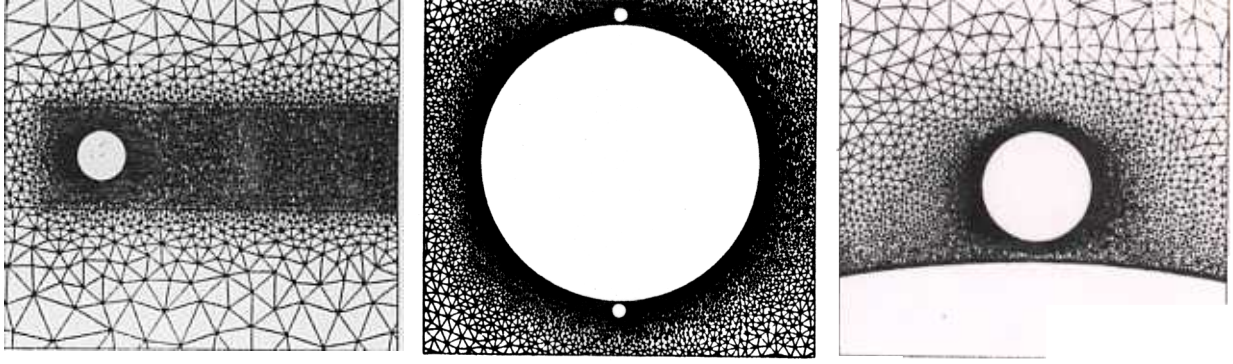

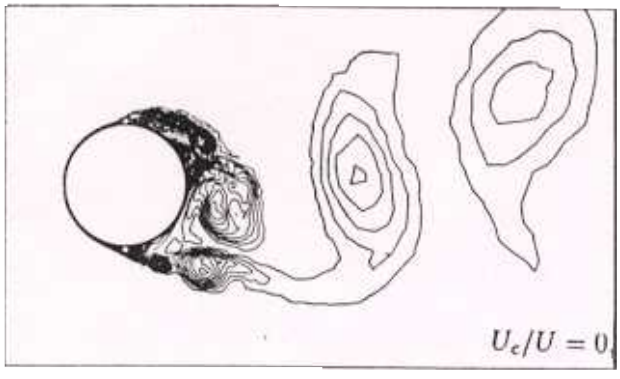

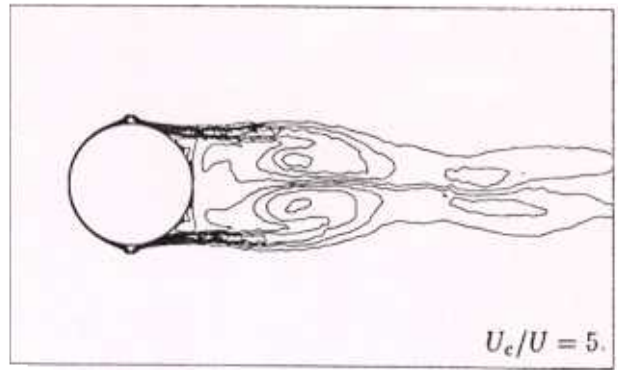

Rotating L.E.

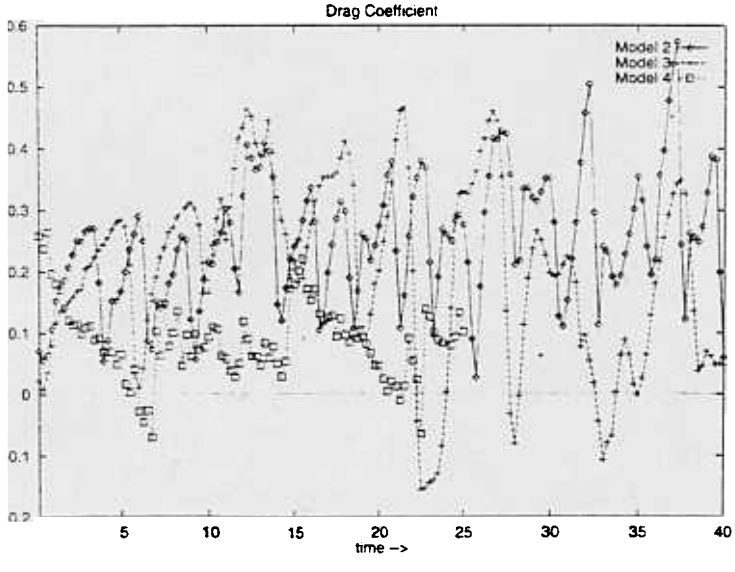

Figure 4. Navier-Stokes solutions for flow control: a) drag reduction for circular cylinder using rotating control cylinders at $Re = 10^4$. Lower figures are for vorticity contours without and with control. b) Drag reduction for NACA 0012 for $\alpha = 20^o$ and $Re = 46,200$ by Robins-Magnus effect. The extent of rotating part for: i) Model 2- 10.49%; Model 3- 16.93% & Model 4- 40.63%.

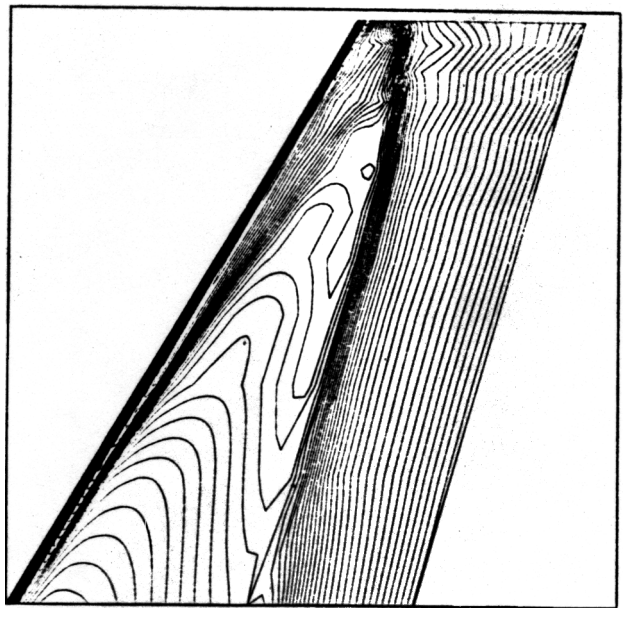

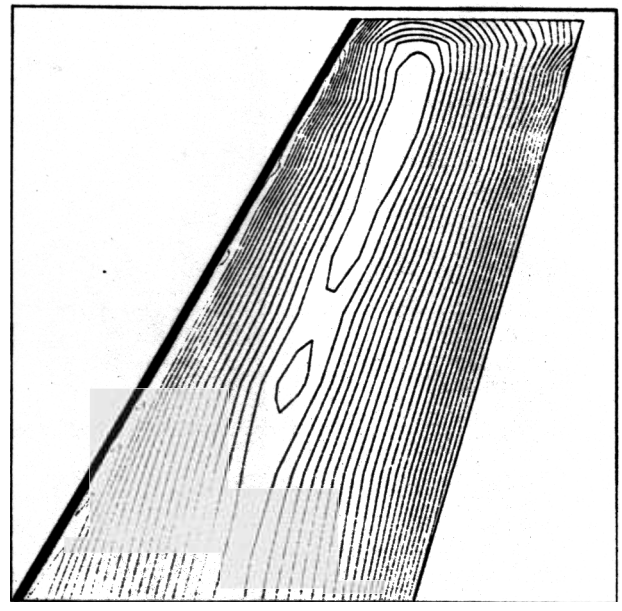

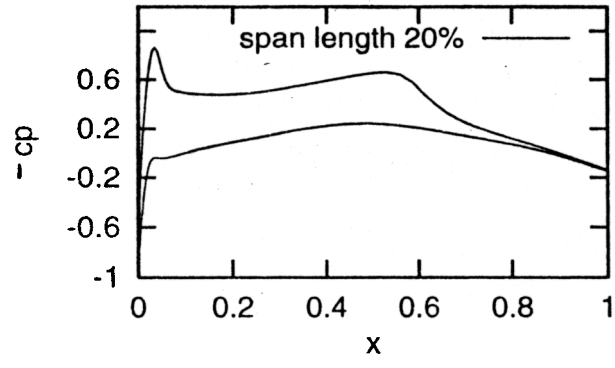

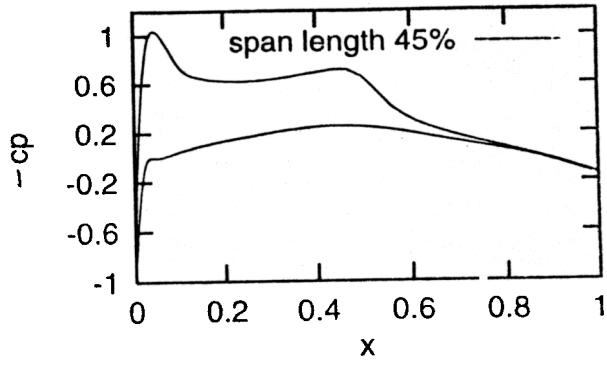

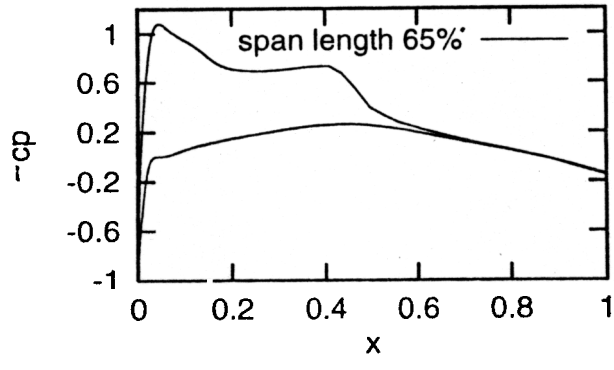

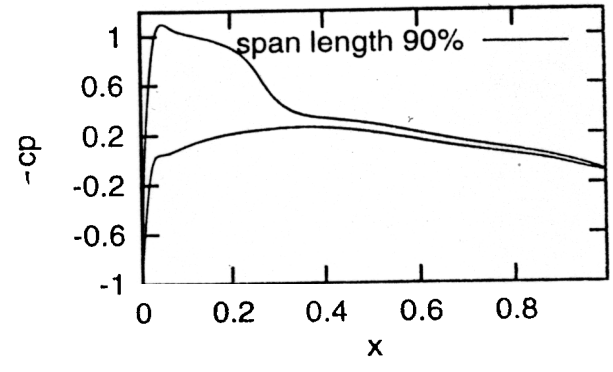

Figure 5. Navier- Stokes solution for flow past ONERA M6 wing for $M = 0.84$ and $Re = 1.2X10^7$ at $\alpha = 3.03^o$. Top left shows pressure contours on upper and top right shows the same for lower surface. Shown below are the C_p plots at various spanwise location.

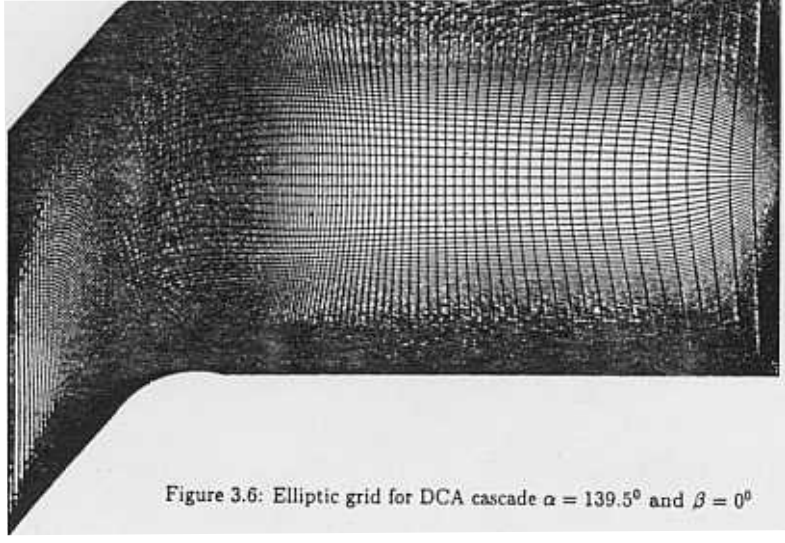

Figure 3.6: Elliptic grid for DCA cascade $\alpha = 139.5^0$ and $\beta = 0^0$

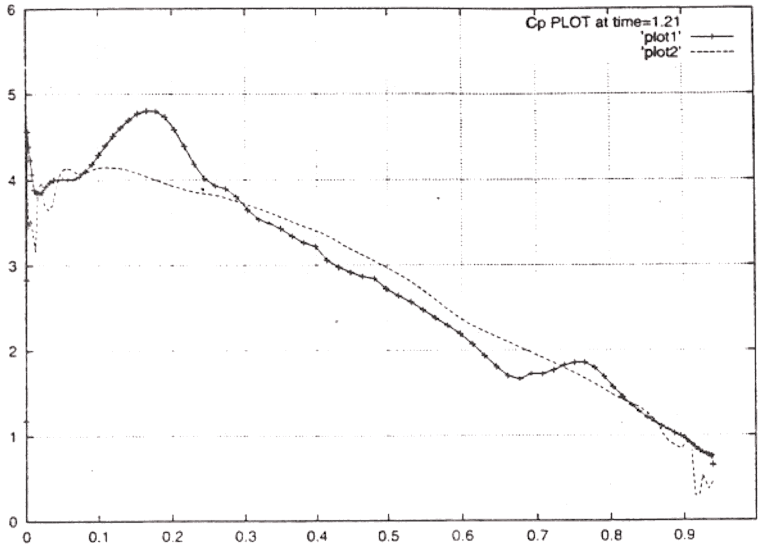

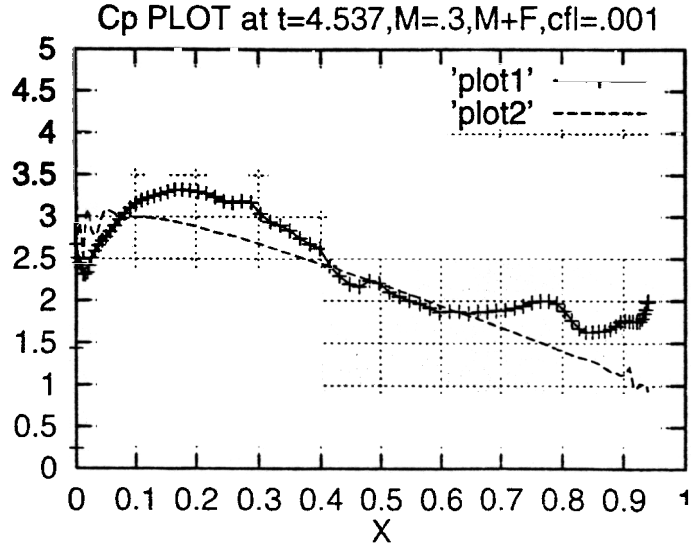

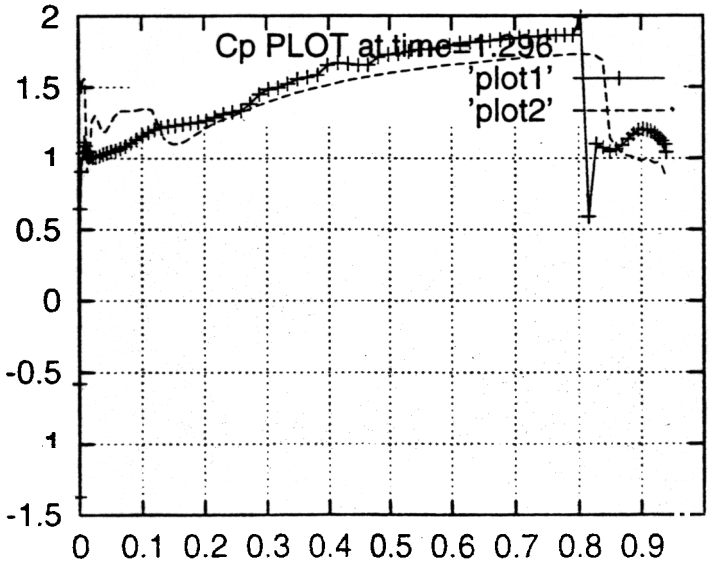

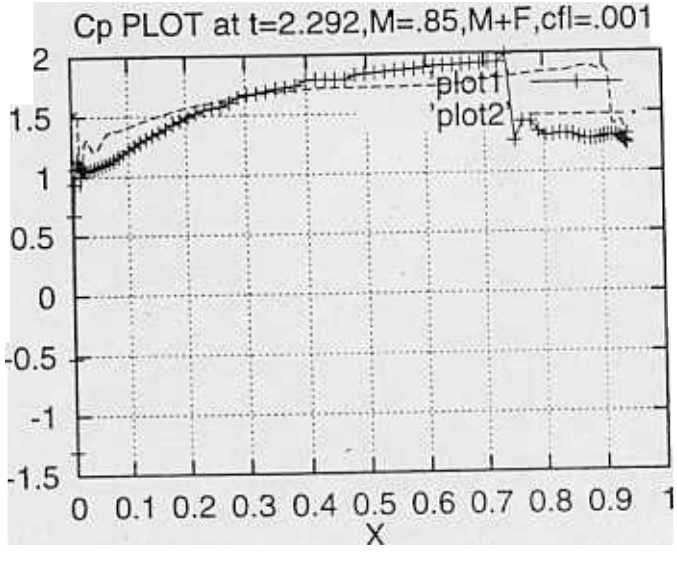

Figure 6. Navier- Stokes solution for flow past DCA cascade for $M = 0.3 and 0.85$ and $Re = 5X10^5$. Top figure shows the grid used.

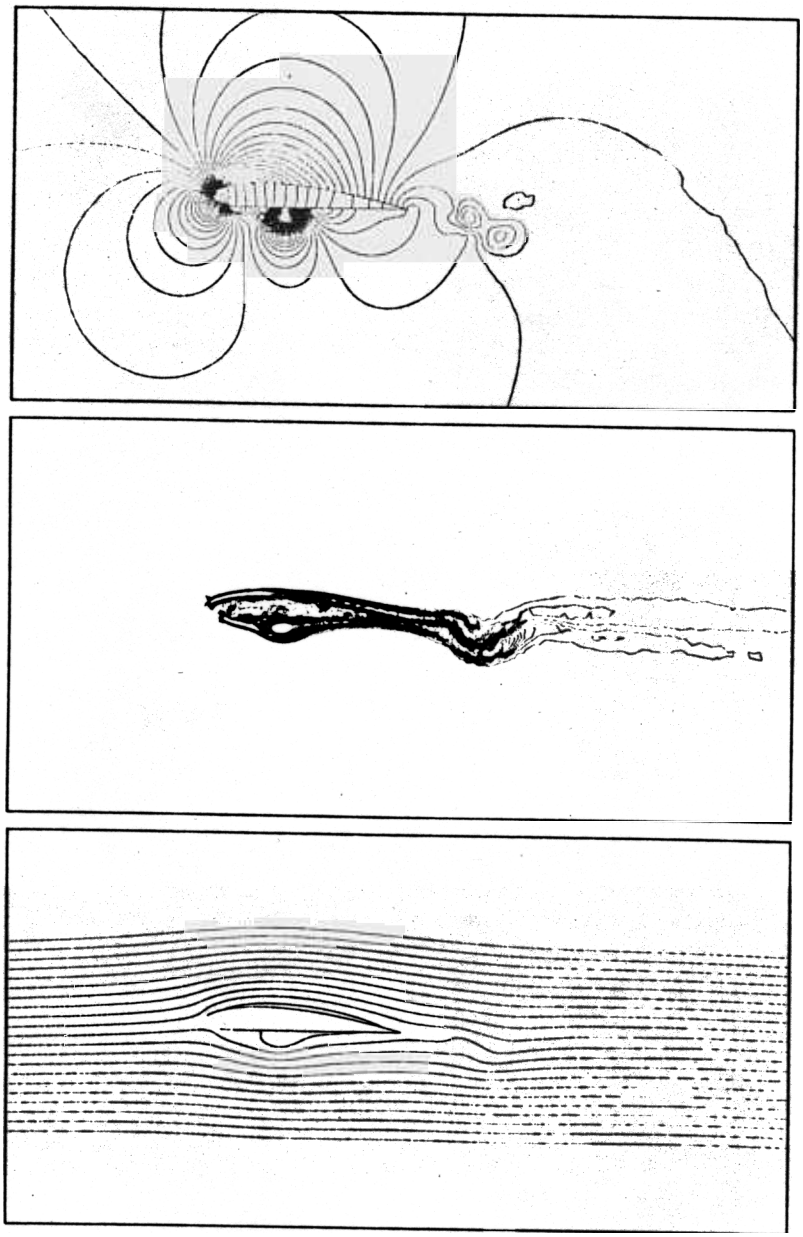

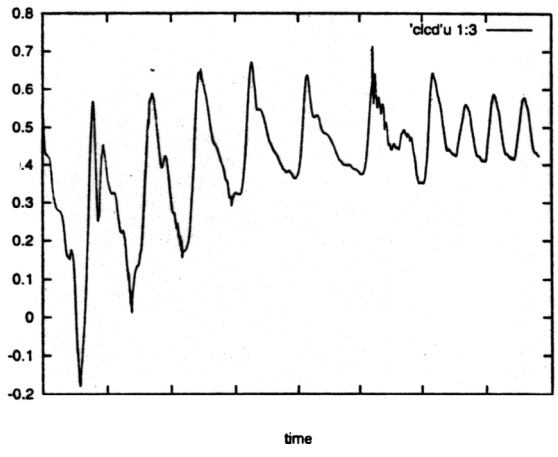

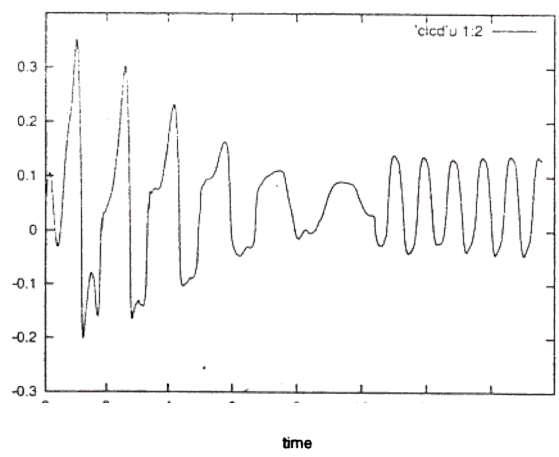

Figure Navier Stokes solution flow past parafoil with Baldwin Lomax closure model (Re 10^6) The basic section 16% Clark Y airfoil

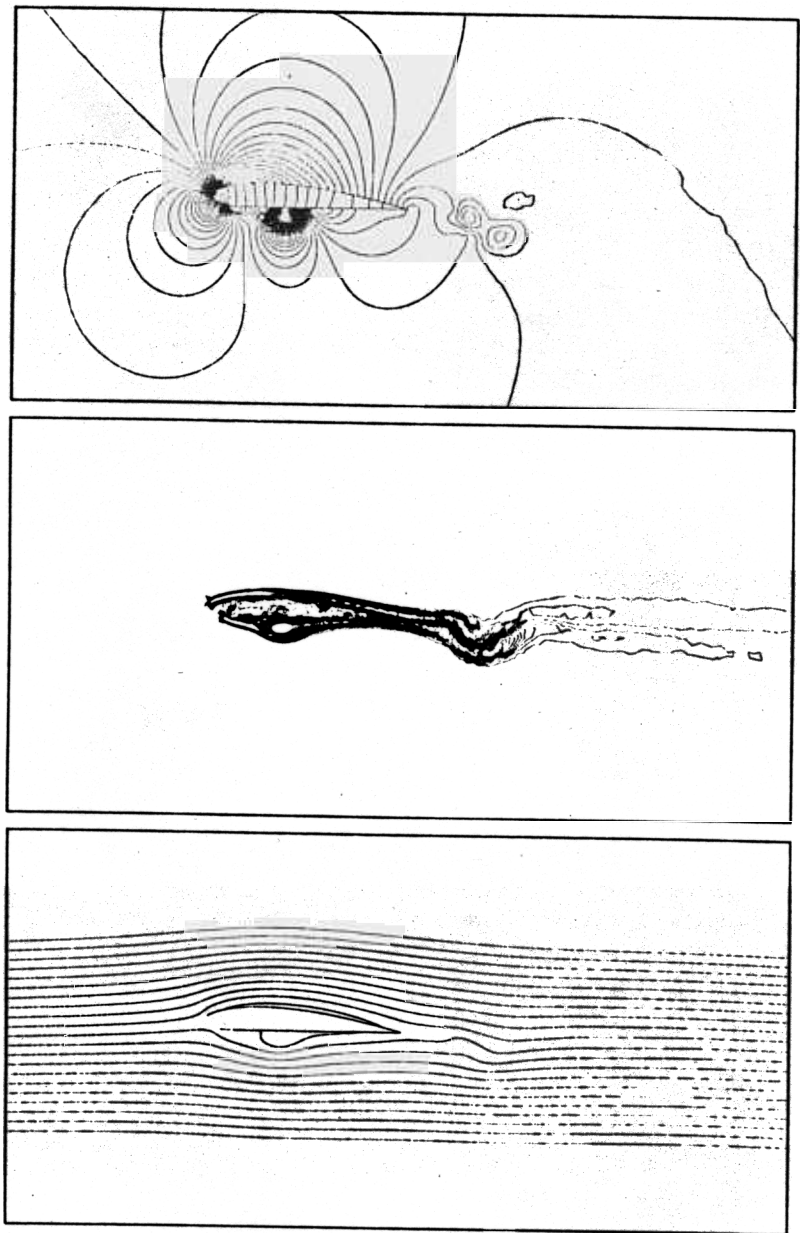

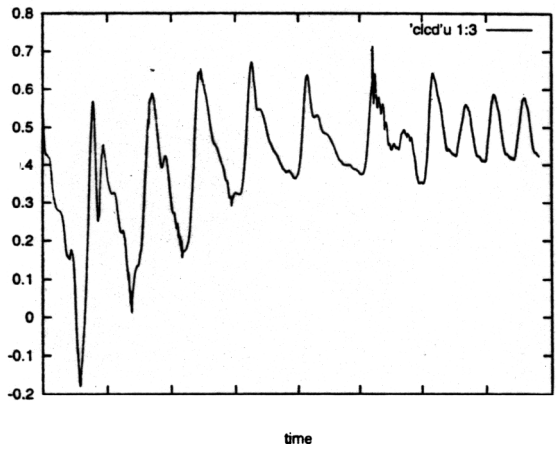

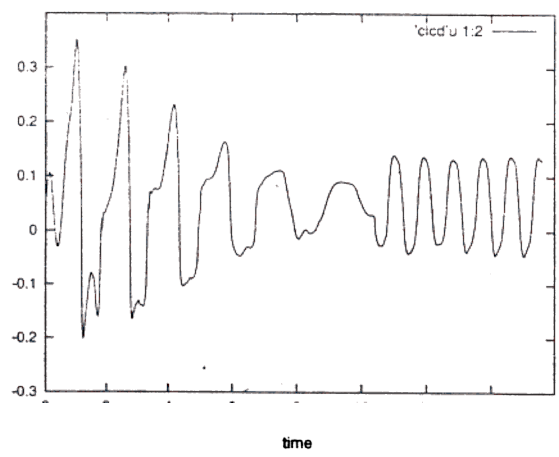

Figure Navier Stokes solution flow past parafoil with Baldwin Lomax closure model (Re 10^6) The basic section 16% Clark Y airfoil

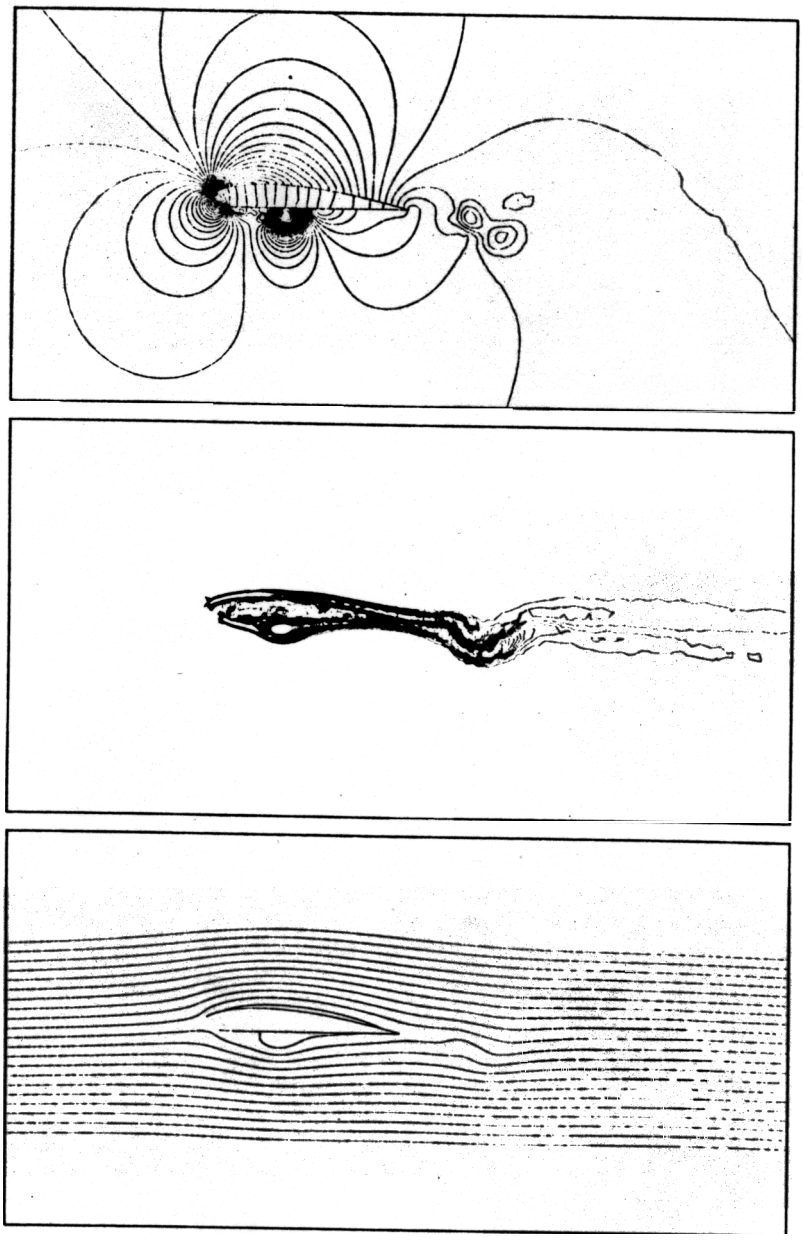

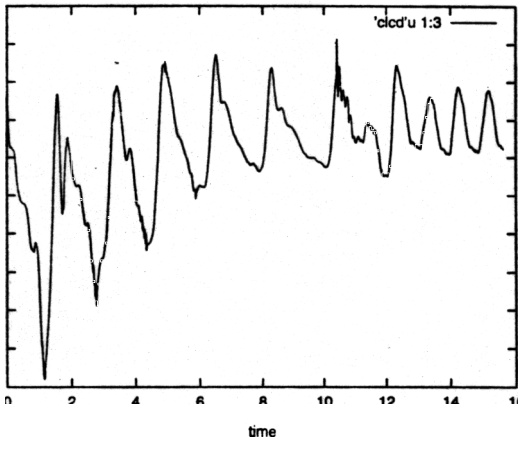

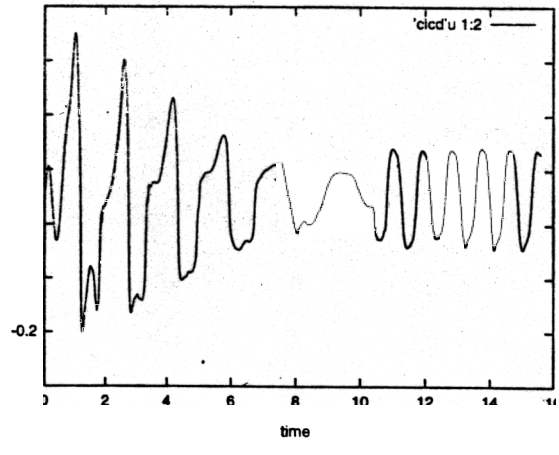

gu ier Stokes for flo past ıafoi ith Lor ıax
mod 10^6 Th basic ion % lark airfo

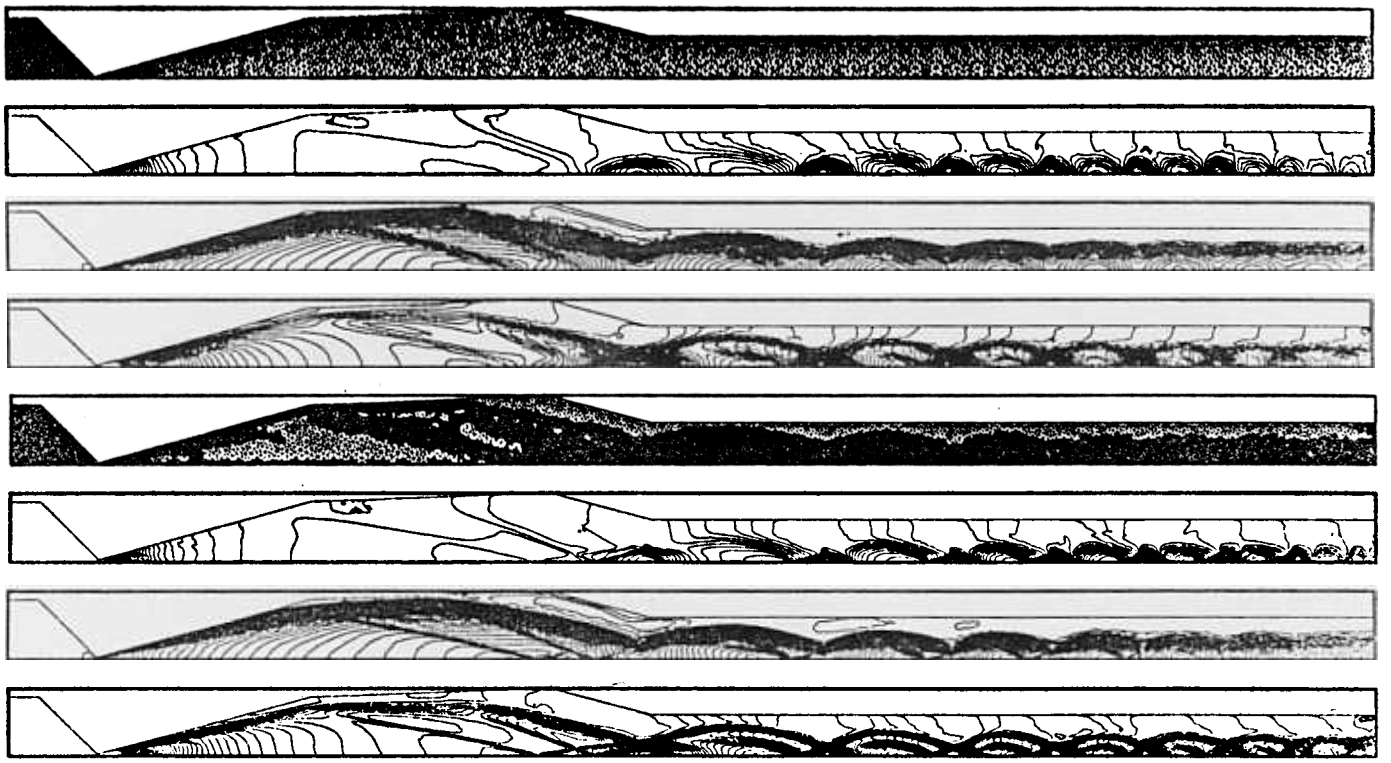

Figure 8a. FE mesh, pressure, Mach number & density fields for the base and refined mesh computed for supersonic wind tunnel with the stagnation to exit pressure ratio 25.

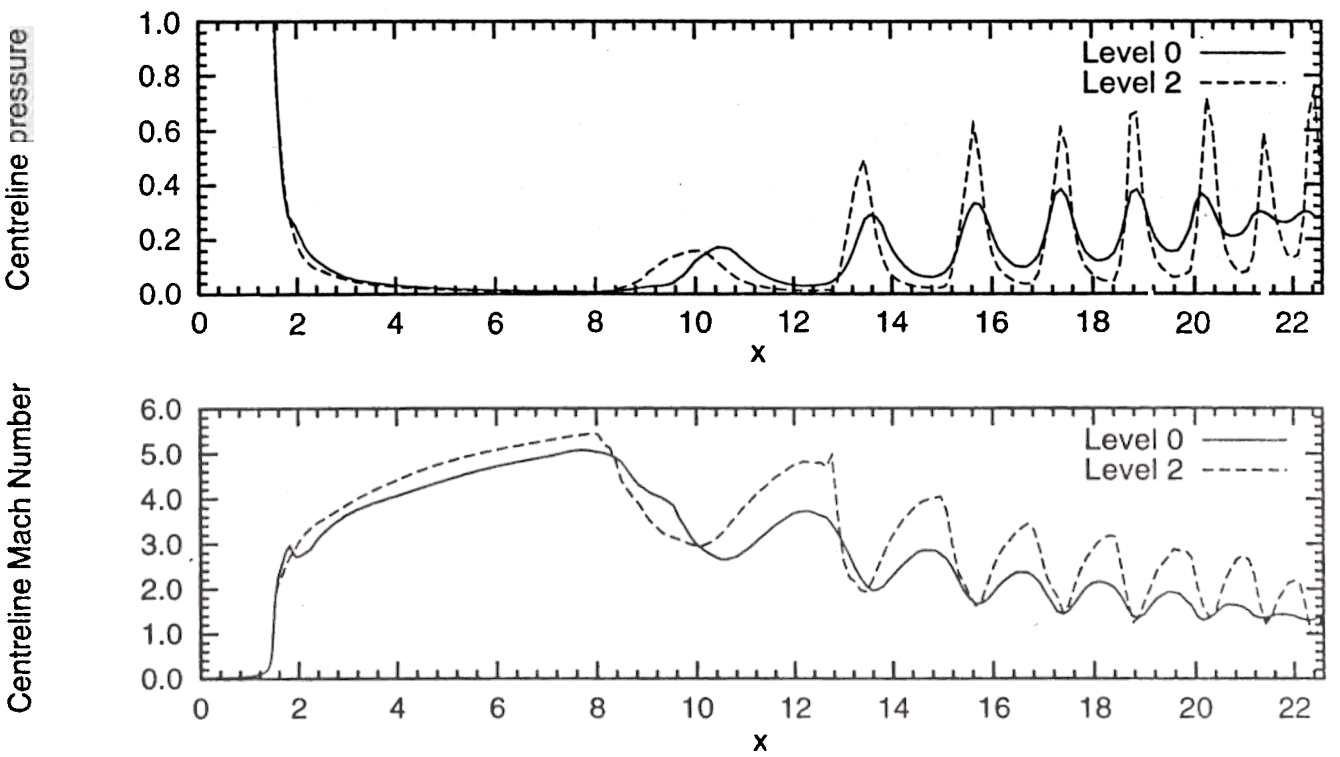

Figure 8b. Centerline pressure and Mach number variation for a supersonic wind tunnel with stagnation to exit pressure ratio of 25.

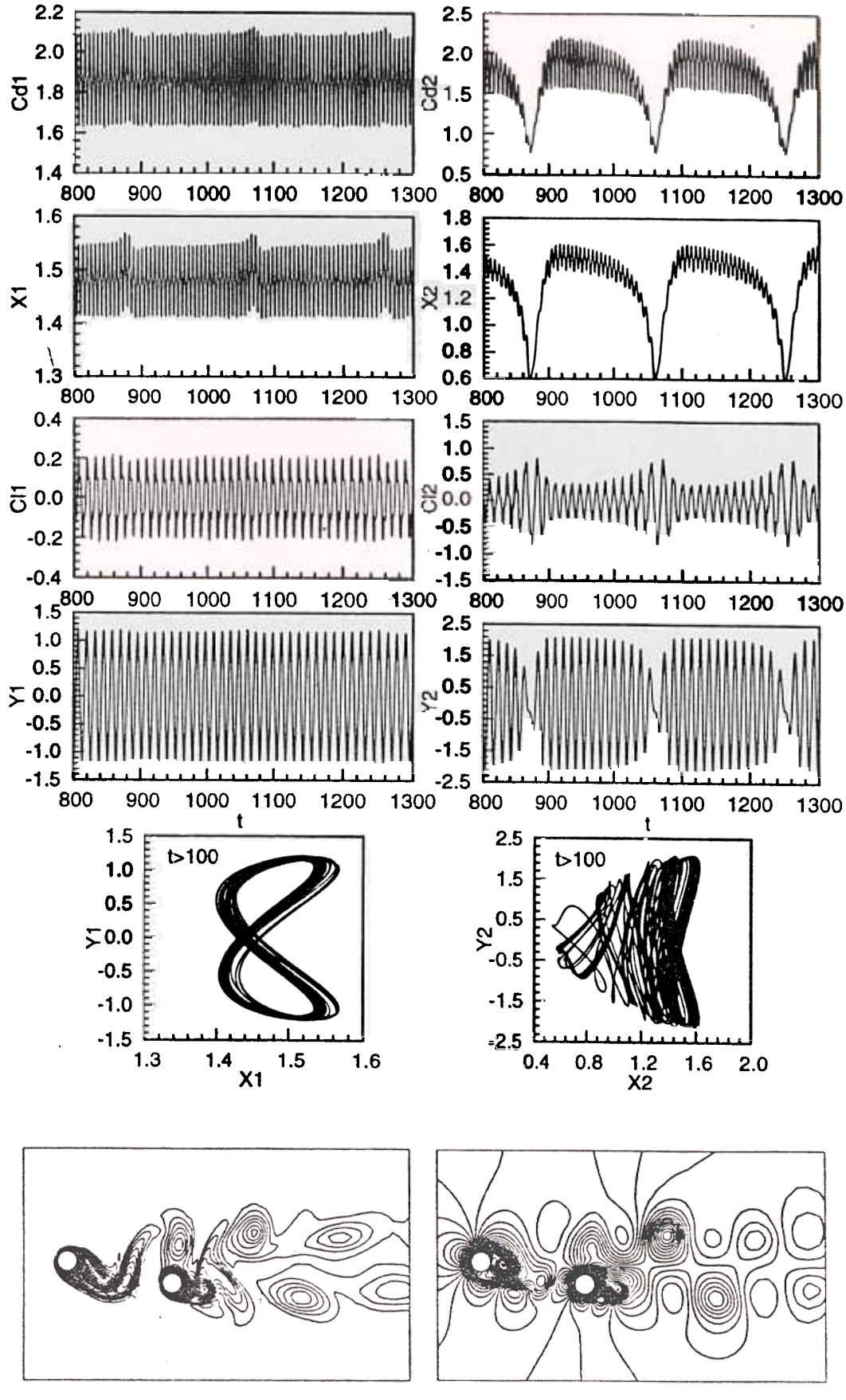

Figure 9. Navier- Stokes solution for flow past two oscillating cylinders at $Re = 100$ mounted on flexible supports and allowed to vibrate under the action of fluid forces. The upper figures show the time histories while the lower one shows the vorticity and pressure fields.

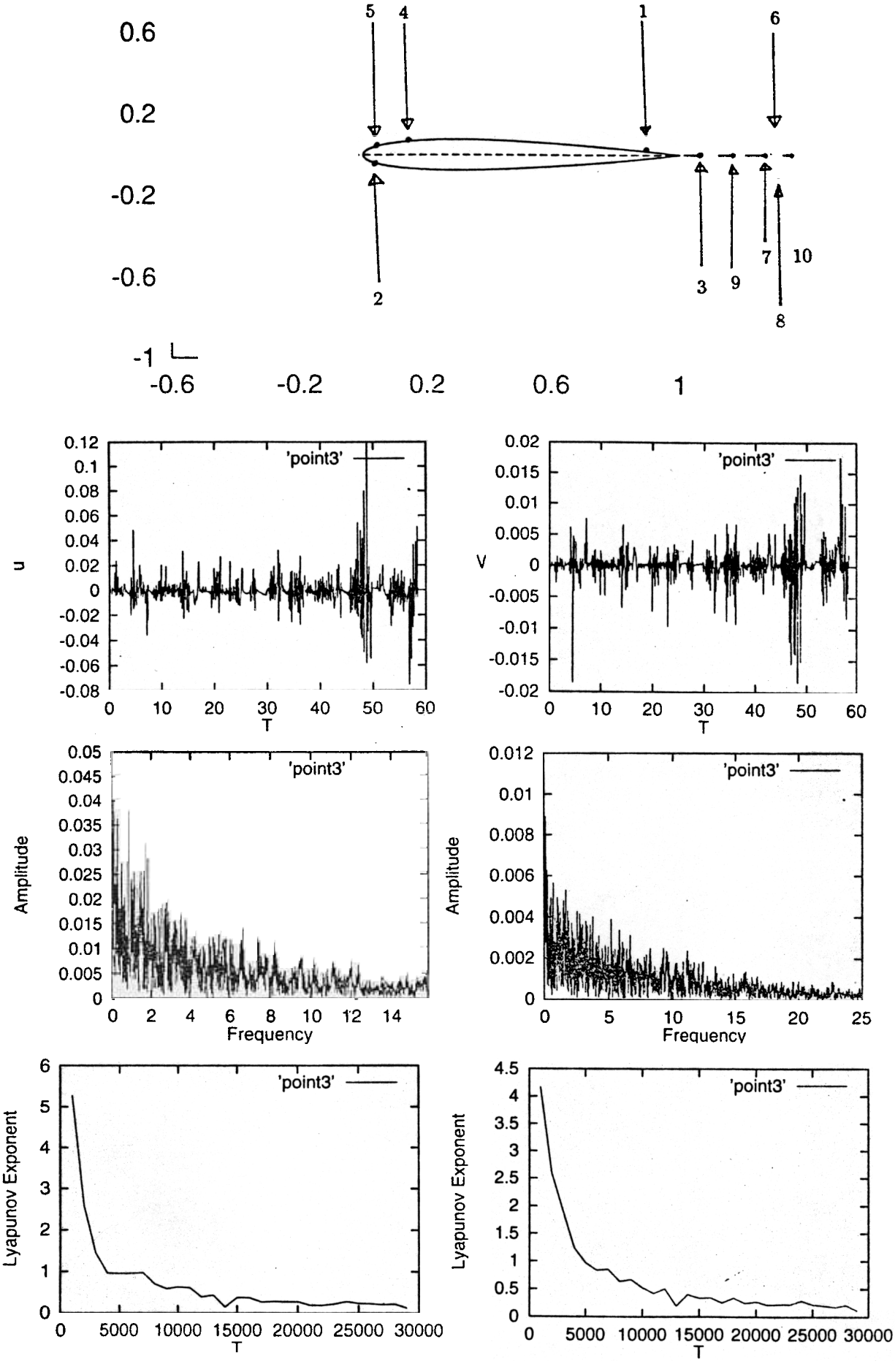

Figure 10. NS solution by 3^{rd} order upwind scheme to study the effect of free stream turbulence (intensity - 5%) on flow past NACA 0015 for $\alpha = 30^{o}$ and $Re = 10^{5}$. Top figure shows the location of sampling points where time series are stored. Also shown are the time series for the third point along with frquency spectrum and Lyapunov plots.

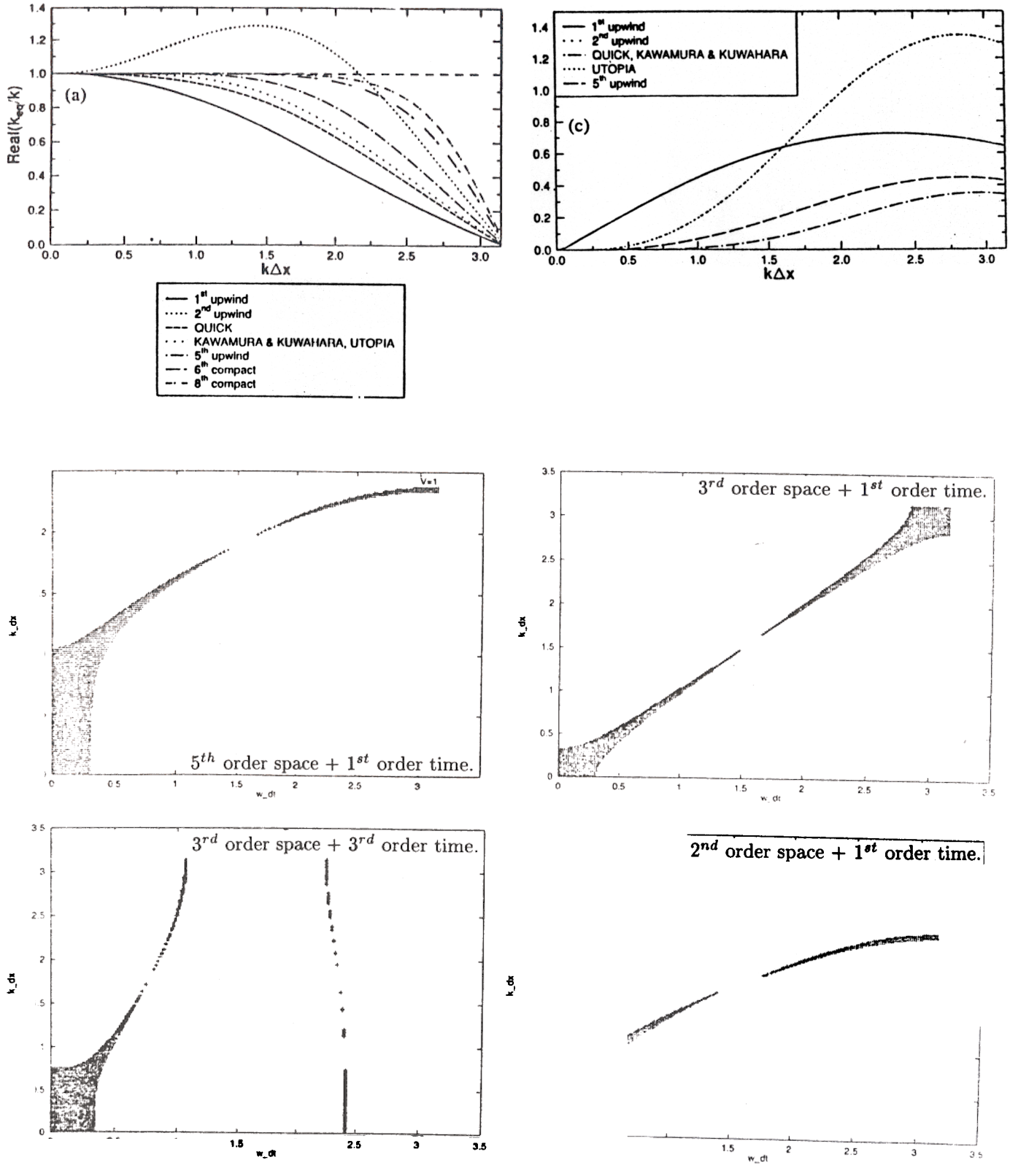

Figure 11. Analysis of various discretization schemes that are used for LES and DNS. Top figures show the real and imaginary part of equivalent wave numbers of the convection terms of NS equation. The bottom figures show the area in $k * \Delta x$ - $\omega * \Delta t$ domain where the dispersion relations are correct up to 5% for wave equation.